

# Niobium segregation in Inconel 718

W. C. LIU, M. YAO

*Department of Materials Science and Engineering, Yanshan University, Qinhuangdao 066004, Hebei, Peoples Republic of China*

Z. L. CHEN, S. G. WANG

*Shenyang Liming Engine Manufacturing Company, Shenyang 110043, Liaoning, Peoples Republic of China*

The segregation of niobium in Inconel 718 was investigated by means of X-ray diffraction. It was found that the very weak and diffuse profiles of sidebands on the lower angle side of  $\gamma$  phase (2 0 0), (2 2 0), (3 1 1), (2 2 2) diffraction peaks were observed in the X-ray diffraction patterns of Inconel 718 cold rolled to 25% reduction, and then solution treated at 1040 °C, 970 °C and aged (DA). The formation of sidebands was contributed to the Nb segregation in the  $\gamma$  matrix. The composition of the Nb rich region was estimated according to the lattice parameter of the Nb rich region. The results showed that the degree of Nb segregation in the matrix is less than that at the grain boundaries. © 1999 Kluwer Academic Publishers

## 1. Introduction

The segregation of niobium at the grain boundaries in Inconel 718 has been studied by X-ray photoelectron spectroscopy, and considerable segregation of niobium, about three to four times higher than that in bulk, was observed at the grain boundaries [1]. The segregation of niobium is responsible for the preferential precipitation of  $\gamma''$  phase at the grain boundaries. Gao and Wei [2] confirmed that the  $\gamma''$  precipitates formed as a result of niobium segregation at the grain boundaries, rather than having the grain boundaries acting simply as the nucleation sites for preferential precipitation. However, aging hardening in this alloy is brought about mainly by the homogeneously nucleated  $\gamma''$  precipitates, which are coherent, disc-shaped particles with {1 0 0} habit and bear the orientation relationship  $\{1\ 0\ 0\}_{\gamma''} // \{1\ 0\ 0\}_{\gamma}$ ;  $[0\ 0\ 1]_{\gamma''} // [0\ 0\ 1]_{\gamma}$  with the host austenite [3–6]. Kirman and Warrington [4] found that the  $\gamma''$  dispersion was sensitive to the excess vacancy concentration of the matrix and that its nucleation was facilitated by the presence of dislocations and extrinsic stacking faults. This effect was contributed to the decrease in the strain energy of a precipitate if the precipitate nucleated at the dislocations and extrinsic faults.

In the previous study [7] the influence of cold rolling on the precipitation of  $\delta$  phase in Inconel 718 aged at 910 °C has been studied. It was found that although the recrystallization had been completed before the precipitation of  $\delta$  phase started, cold rolling still promoted the precipitation of  $\delta$  phase, which might depend on the segregation of niobium at the dislocations. The segregation of niobium in the matrix has been reported by He *et al.* [8]. They observed a stacking fault with a series of cross fringes in Inconel 718 and suggested niobium atoms segregating on (1 1 1) plane of the matrix. The formation of a series of parallel Moir's fringes was due

to the difference in lattice parameters between the thin crystal produced by the segregated niobium atoms and the matrix.

Niobium obviously raises the lattice parameter of  $\gamma$  phase in Inconel 718, and the coefficient of niobium that affects the lattice parameter of  $\gamma$  phase is 0.0624 nm per atomic percent [9]. If niobium segregates in the matrix, the diffraction peaks of the Nb rich regions are separated from those of the  $\gamma$  matrix because of the difference in their lattice parameters. Moreover, the higher atomic scattering ability of niobium provides the condition for determining the segregation of niobium by X-ray diffraction. Therefore, the aim of this paper is to investigate the segregation of niobium in the matrix by X-ray diffraction.

## 2. Experimental

The chemical composition of Inconel 718 is shown in Table I. The 20 mm diameter bars were cold rolled to the strips of 10 mm thickness. These strips were solution treated at 970 °C for 1 hour followed by an air cool, and then were cold rolled to 25% reduction in thickness in multiple passes. The cold rolled samples were given the following heat treatment: solution treatment at (A) 1040 °C and (B) 970 °C for 0.5 hours, followed by an air cool and then aged at 720 °C for 8 hours, a furnace cool at 55 °C/hour to 620 °C where they were held for 8 hours, followed by an air cool to room temperature (DA).

The samples for X-ray diffraction were prepared by mechanical polishing followed by chemical etching. The X-ray diffraction patterns were obtained on a D/mas-rB X-ray diffractometer with  $\text{CuK}\alpha$  radiation. The lattice constant of  $\gamma$  phase was calculated with the Nelson-Riley extrapolation method.

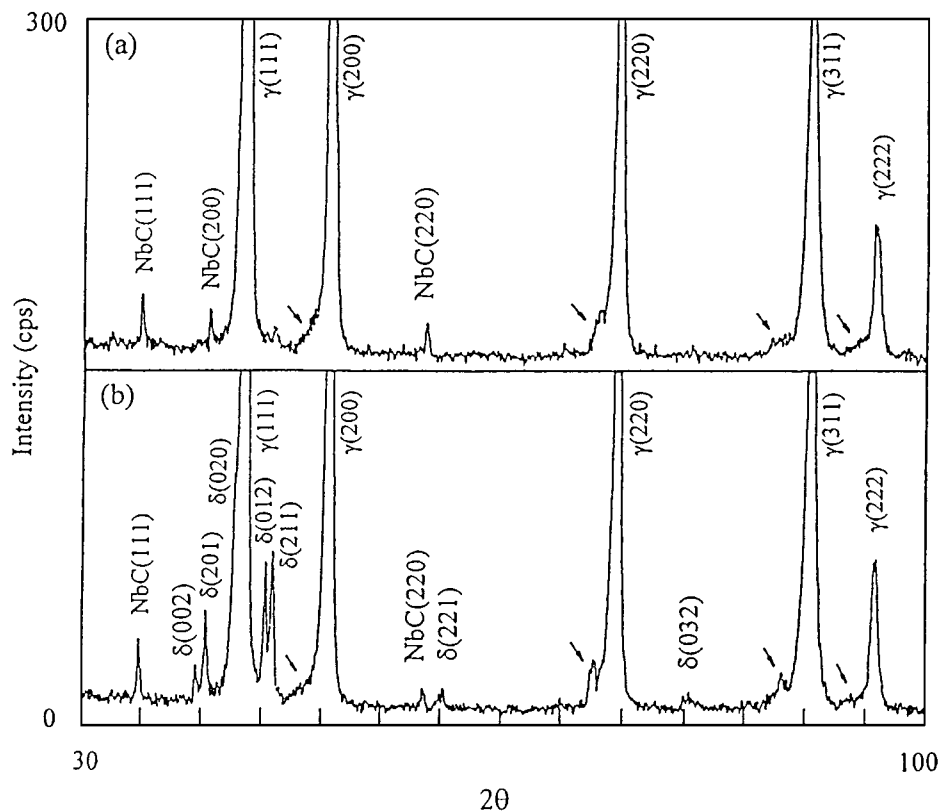


Figure 1 X-ray diffraction patterns of Inconel 718 solution treated at (a) 1040 °C and (b) 970 °C and then aged (DA).

TABLE I Chemical composition of Inconel 718 (wt %)

C	Ni	Cr	Nb	Mo	Ti	Al	Mn	Si	P	S	Fe
0.04	52.52	18.34	5.10	3.07	1.00	0.50	0.02	0.11	0.004	0.002	Bal.

### 3. Results and discussion

#### 3.1. The segregation of niobium

Fig. 1 shows the diffraction patterns of Inconel 718 which is solution treated at 1040 and 970 °C, and then aged. The  $\gamma$  phase (1 1 1), (2 0 0), (2 2 0), (3 1 1), (2 2 2), NbC (1 1 1), (2 0 0), (2 2 0), and  $\delta$  phase (0 0 2), (2 0 1), (0 2 0), (0 1 2), (2 1 1), (2 2 1), (0 3 2) diffraction peaks can be observed. Moreover, the very weak and diffuse profiles of sidebands on the lower angle side of the  $\gamma$  phase (2 0 0), (2 2 0), (3 1 1), (2 2 2) diffraction peaks can be observed. The overlapping peaks can be separated by the computer. The diffraction angles of  $\gamma$  phase and their sidebands are listed in Table II.

When the specimen is solution treated 1040 °C for 0.5 hours and then aged (DA), its microstructure consists

of the  $\gamma$  phase,  $\gamma''$ ,  $\gamma'$  phases and NbC. The  $\gamma''$  phase is DO<sub>22</sub> structure, and the  $\gamma'$  phase is L1<sub>2</sub> structure [3–6]. The lattice parameter of  $\gamma''$  phase is  $a = 0.3624$  nm and  $c = 0.7406$  nm, and the lattice parameter of  $\gamma'$  phase is 0.3590 nm [5]. The diffraction plane, interplanar spacing, diffraction angle and relative intensity of  $\gamma''$ ,  $\gamma'$  phases are given in Table III. By comparison of the position of sidebands (Table II) and the position of  $\gamma''$  phase diffraction peaks (Table III), the formation of sidebands can not be contributed to the  $\gamma''$  phase. In addition, we can not observe the  $\gamma'$  phase (2 1 0)<sup>s</sup>, (2 1 1)<sup>s</sup>, (3 0 0)<sup>s</sup>, (3 1 0)<sup>s</sup> diffraction peaks in the patterns because of their weak intensities. Therefore, the formation of sidebands can not be caused by the  $\gamma'$  phase. Although we can not observe the sideband on the lower angle side of the  $\gamma$  phase (1 1 1) diffraction peak, the distribution of the profile of sidebands suggests that the micro austenite region is present in the  $\gamma$  matrix. The reason why we can not observe the (1 1 1) diffraction peak of the micro austenite region is possibly due to the broadening of the  $\gamma$  phase (1 1 1) diffraction peak caused by the  $\gamma''$  phase (1 1 2) diffraction peak. If

TABLE II The diffraction angle (2 $\theta$ ) of the  $\gamma$  matrix and the Nb rich region in solution treated and aged Inconel 718

Diffraction plane	Diffraction angle 2 $\theta$ (°)			
	A: 1040 °C/0.5 h + DA		B: 970 °C/0.5 h + DA	
	The $\gamma$ matrix	The Nb rich region	The $\gamma$ matrix	The Nb rich region
(111)	43.47	—	43.48	—
(200)	50.54	49.05	50.57	48.92
(220)	74.50	73.15	74.54	72.72
(311)	90.40	87.76	90.46	87.74
(222)	95.81	94.34	95.85	93.98

TABLE III Diffraction plane ( $hkl$ ), interplanar spacing ( $d$ ), diffraction angle ( $2\theta$ ) and relative intensity ( $I$ ) of  $\gamma''$  and  $\gamma'$  phases

The $\gamma''$ phase				The $\gamma'$ phase			
$hkl$	$d$	$2\theta$	$I$	$hkl$	$d$	$2\theta$	$I^a$
101	3.262	27.34	5	100 <sup>s</sup>	3.600	24.73	W
110	2.561	35.04	1	110 <sup>s</sup>	2.546	35.26	W
112	2.107	42.92	100	111	2.079	43.54	VS
103	2.040	44.41	—	200	1.800	50.72	S
004	1.852	49.20	16	210 <sup>s</sup>	1.610	57.22	VW
200	1.812	50.36	31	211 <sup>s</sup>	1.470	63.28	VW
202	1.627	56.57	1	220	1.273	74.56	S
211	1.587	58.13	1	300 <sup>s</sup>	1.200	79.95	VW
204	1.294	73.13	18	310 <sup>s</sup>	1.138	85.25	VW
220	1.286	73.66	—	311	1.085	90.51	S
310	1.150	84.19	—	222	1.039	95.77	W
400	0.906	116.62	—	400	0.900	117.87	W

<sup>a</sup>VS: very strong, S: strong, W: weak, VW: very weak.

TABLE IV The lattice parameters of the  $\gamma$  matrix and the Nb rich region

Heat treatment	The lattice parameter (nm)	
	The $\gamma$ matrix	The Nb rich region
A: 1040/0.5 h + DA	0.3598	0.3646
B: 970/0.5 h + DA	0.3597	0.3636

we take into account the effect of the (1 1 1) diffraction peak of the micro austenite region, the lattice parameters of the  $\gamma$  matrix and the micro austenite region calculated with the Nelson-Riley extrapolation method are given in Table IV. Since the lattice parameter of the micro austenite region is higher than that of the  $\gamma$  matrix, the micro austenite region can be contributed to the segregation of alloying elements. Pang [1] has determined the chemical composition at the grain boundaries by X-ray photoelectron spectroscopy, and found the niobium content at the grain boundary was about three to four times higher than that in the  $\gamma$  matrix. As long as niobium can segregate at the grain boundaries, niobium can segregate at excess vacancy, dislocations and extrinsic stacking faults in the  $\gamma$  matrix. Therefore, the micro austenite region is actually the niobium rich region.

### 3.2. The composition in the Nb rich region

The lattice parameter of  $\gamma$  phase is dependent on alloying elements in the  $\gamma$  phase and the amount of alloying elements. The effect of alloying elements on the lattice parameter of  $\gamma$  phase increases in sequence of Co, Fe, Cr, Al, Ti, Mo, W, Nb in Ni-based superalloy. For Inconel 718, the relationship between the lattice parameter of  $\gamma$  phase ( $a$ ) and the content of alloying elements in the  $\gamma$  phase is given by [9]

$$a = 0.35234 + 0.0119D_{Fe} + 0.013D_{Cr} + 0.0183D_{Al} + 0.036D_{Ti} + 0.0421D_{Mo} + 0.0624D_{Nb} \quad (1)$$

where  $D_i$  is the content of the alloying element  $i$  (at %) in the  $\gamma$  phase. For the sample solution treated at

TABLE V The compositions of Inconel 718 [1] and the grain boundary determined by Pang [1]

Comments: composition	Ni	Cr	Fe	Nb	Mo	Ti	Al
Alloy composition	52.8	21.1	18.6	3.0	1.7	1.1	0.9
Grain boundary composition	49.1	18.9	15.0	12.3	4.7	—	—

1040 °C and then aged, the  $\delta$ ,  $\gamma''$  and  $\gamma'$  phases have been fully solutioned, and the measured lattice parameter of  $\gamma$  phase is 0.36077 nm. During aging at lower temperature after solution treatment, the lattice parameter of  $\gamma$  phase decreases with aging time [10, 11] because the formation of  $\gamma''$  and  $\gamma'$  phases decreases the content of alloying elements in the  $\gamma$  phase. Under the standard aging thermal treatment condition (DA), the measured lattice parameter of the  $\gamma$  matrix is 0.3598 nm. However, the lattice parameter of the Nb rich region is 0.3646 nm, which is markedly higher than that of the  $\gamma$  matrix. The increase of the lattice parameter of the Nb rich region reflects the segregation degree of alloying elements. Therefore, the lattice parameter of the Nb rich region can be used to estimate the composition in the Nb rich region. The grain boundary composition (at %) determined by Pang [1] is given in Table V. Assuming that the ratio of the degree of Cr, Fe, Nb, Mo segregation in the  $\gamma$  matrix to that at the grain boundaries is constant and the degree of Al, Ti segregation is equal to that of Mo segregation, we can give the following equation:

$$(0.2042 - D_{Cr})/0.2042 = \alpha(0.211 - 0.189)/0.211 \quad (2)$$

$$(0.2000 - D_{Fe})/0.2000 = \alpha(0.186 - 0.150)/0.186 \quad (3)$$

$$(D_{Nb} - 0.0318)/0.0318 = \alpha(0.123 - 0.030)/0.030 \quad (4)$$

$$(D_{Mo} - 0.0185)/0.0185 = \alpha(0.047 - 0.017)/0.017 \quad (5)$$

$$(D_{Ti} - 0.0121)/0.0121 = (D_{Mo} - 0.0185)/0.0185 \quad (6)$$

$$(D_{Al} - 0.0107)/0.0107 = (D_{Mo} - 0.0185)/0.0185 \quad (7)$$

where  $\alpha$  is constant. Substituting Equations 2 to 7 and the lattice parameter of the Nb rich region into Equation 1, we can calculate the contents of alloying elements in the Nb rich region. The results are shown in Table VI. It is noted that the degree of Nb segregation in the matrix is less than that at the grain boundaries.

### 3.3. The composition of the $\gamma$ matrix

During aging after solution treatment, the composition of the  $\gamma$  matrix changes because of the formation of  $\delta$ ,  $\gamma''$  and  $\gamma'$  phases. The contents of alloying elements in the  $\gamma$  phase depend on the compositions and contents of  $\delta$ ,  $\gamma''$  and  $\gamma'$  phases. If neglecting the Nb segregation, the content of alloying element  $i$  in the  $\gamma$  phase as a function of the compositions and contents of  $\delta$ ,  $\gamma''$  and  $\gamma'$  phases can be given by following equation [9]:

TABLE VI Compositions of this alloy, The Nb rich region, the  $\gamma$  matrix and the  $\delta$ ,  $\gamma''$ ,  $\gamma'$  phases (at %)

Comments: composition	Ni	Cr	Fe	Nb	Mo	Ti	Al
Alloy composition	52.08	20.42	20.00	3.18	1.85	1.21	1.07
Nb rich region in A specimen	46.88	19.39	18.12	7.96	3.43	2.24	1.98
Nb rich region in B specimen	45.47	19.12	17.63	9.21	3.84	2.51	2.22
$\gamma$ matrix in A specimen	50.47	22.77	22.24	0.96	1.96	0.65	0.95
$\gamma$ matrix in B specimen	50.26	23.06	22.46	0.64	1.93	0.67	0.98
$\delta$ phase [12]	64.90	3.4	5.3	20.4	2.2	3.0	0.80
$\gamma''$ phase [12]	66.87	0.76	0.86	25.1	1.05	4.92	0.44
$\gamma'$ phase [12]	69.35	0.5	2.15	10.2	0.40	9.40	8.00

$$D_i = \frac{C_i/W_i - b_i W_\delta / (\sum b_i W_i) - d_i W_{\gamma''} / (\sum d_i W_i) - e_i W_{\gamma'} / (\sum e_i W_i)}{\sum C_i/W_i - W_\delta / (\sum b_i W_i) - W_{\gamma''} / (\sum d_i W_i) - W_{\gamma'} / (\sum e_i W_i)} \quad (8)$$

where  $W_\delta$ ,  $W_{\gamma''}$ ,  $W_{\gamma'}$  are the weight percentages of  $\delta$ ,  $\gamma''$  and  $\gamma'$  phases, respectively.  $C_i$  is the content of alloying element  $i$  in this alloy in wt %.  $W_i$  is the atomic weight of element  $i$ .  $b_i$ ,  $d_i$ ,  $e_i$  are the content of alloying element  $i$  in the  $\delta$ ,  $\gamma''$  and  $\gamma'$  phases in at %, respectively. The compositions of  $\delta$ ,  $\gamma''$  and  $\gamma'$  phases determined by Burke [12] are listed in Table VI. The weight percentages of  $\delta$ ,  $\gamma''$ ,  $\gamma'$  phases and NbC have been determined by X-ray diffraction technique for the solution treated and then aged samples [13], as shown in Table VII. Thus we can calculate the composition of the  $\gamma$  matrix by means of Equation 8. The results are given in Table VI. It has been found that the content of Nb in the  $\gamma$  matrix is very low because of the formation of  $\delta$ ,  $\gamma''$ ,  $\gamma'$  phases. If there is not the segregation of Nb in the  $\gamma$  matrix, it is difficult for the  $\gamma''$  and  $\gamma'$  phases to precipitate further in the  $\gamma$  matrix. It is obvious that the segregation of Nb in the  $\gamma$  matrix facilitate the precipitation of  $\gamma''$  and  $\gamma'$  phases.

#### 4. Conclusion

The very weak and diffuse profiles of sidebands on the lower angle side of  $\gamma$  phase (200), (220), (311), (222) diffraction peaks were observed in the X-ray diffraction patterns of solution treated and aged Inconel

718. The formation of sidebands was contributed to the Nb segregation in the  $\gamma$  matrix. The lattice parameter of the Nb rich region is higher than that of the  $\gamma$  matrix. The composition of the Nb rich region was estimated according to the lattice parameter of the Nb rich region. The results showed that the degree of Nb segregation in the matrix is less than that at the grain boundaries.

#### References

1. X. J. PANG, D. J. DWYER, M. GAO, P. VALERIO and R. P. WEI, *Scripta Met. et Mater.* **31** (1994) 345.
2. M. GAO and R. P. WEI, *ibid.* **32** (1995) 987.
3. D. F. PAULONIS, J. M. OBLAK and D. S. DUVALL, *Trans. ASM* **62** (1969) 611.
4. I. KIRMAN and D. H. WARRINGTON, *Metall. Trans.* **1A** (1970) 2667.
5. R. COZAR and A. PINEAU, *ibid.* **4A** (1973) 47.
6. M. SUNDARARAMAN, P. MUKHOPADHYAY and S. BANERJEE, *ibid.* **23A** (1992) 2015.
7. W. C. LIU, F. R. XIAO, M. YAO and Z. L. CHEN, *Scripta Mater.* **37** (1997) 53.
8. J. H. HE, S. FUKUYAMA and K. YOKOGAWA, *Scripta Met. et Mater.* **31** (1994) 1421.
9. W. C. LIU, F. R. XIAO, M. YAO and Z. L. CHEN, *Scripta Mater.* **37** (1997) 59.
10. K. KUSABIRAKI, S. IKEUCHI and T. OOKA, *Mater. Trans. JIM* **37** (1996) 1050.
11. C. SLAMA, C. SERVANT and G. CIZERON, *J. Mater. Res.* **12** (1997) 2298.
12. M. G. BURKE and M. K. MILLER, in "Superalloys 718, 625, 706 and Various Derivatives," edited by E. A. Loria (TMS, Warrendals, PA, 1991) p. 337.
13. W. C. LIU, F. R. XIAO, M. YAO and Z. L. CHEN, *J. Mater. Sci. Lett.* **16** (1997) 769.

TABLE VII The contents of NbC,  $\delta$ ,  $\gamma''$ ,  $\gamma'$  phases (wt %) in Inconel 718 solution treated at 1040 and 970 °C and then aged (DA) [13]

Heat treatment	$W_{\text{NbC}}$	$W_\delta$	$W_{\gamma''}$	$W_{\gamma'}$	$W_\gamma$
A: 1040/0.5 h + DA	0.49	0.25	9.39	2.35	87.52
B: 970/0.5 h + DA	0.50	4.02	7.80	1.95	85.73

Received 20 April  
and accepted 23 December 1998